# Selection of high-affinity Centyrin FN3 domains from a simple library diversified at a combination of strand and loop positions

**Michael D.Diem, Linus Hyun, Fang Yi, Randi Hippensteel, Elise Kuhar, Cassandra Lowenstein, Edward J.Swift, Karyn T.O'Neil and Steven A. Jacobs[1]**

Janssen Research & Development, L.L.C., 1400 McKean Road, PO Box 776, Spring House, PA 19477, USA

[1]To whom correspondence should be addressed.
E-mail: sjacobs9@its.jnj.com

**Alternative scaffold molecules represent a class of proteins important to the study of protein design and mechanisms of protein–protein interactions, as well as for the development of therapeutic proteins. Here, we describe the generation of a library built upon the framework of a consensus FN3 domain sequence resulting in binding proteins we call Centyrins. This new library employs diversified positions within the C-strand, CD-loop, F-strand and FG-loop of the FN3 domain. CIS display was used to select high-affinity Centyrin variants against three targets; c-MET, murine IL-17A and rat TNFα and scanning mutagenesis studies were used to define the positions of the library most important for target binding. Contributions from both the strand and loop positions were noted, although the pattern was different for each molecule. In addition, an affinity maturation scheme is described that resulted in a significant improvement in the affinity of one selected Centyrin variant. Together, this work provides important data contributing to our understanding of potential FN3 binding interfaces and a new tool for generating high-affinity scaffold molecules.**

*Keywords*: consensus/FN3/library/scaffold

## Introduction

A major goal of the biopharmaceutical industry is the discovery of agents capable of disrupting protein–protein interactions for therapeutic purposes. Protein-based therapeutics are the preferred molecules for inhibition of extracellular protein–protein interactions, with monoclonal antibodies (mAbs) most often the agent of choice due to their exquisite affinity and specificity (Pavlou and Reichert, 2004; Reichert and Pavlou, 2004; Sliwkowski and Mellman, 2013). In addition to the use of mAbs, a new class of therapeutic proteins, termed alternative scaffolds, has emerged. Scaffold proteins are designed to bind to targets with the high affinity and specificity normally characteristic of mAbs. This binding however is accomplished using three-dimensional structures and surfaces significantly different than those of the mAb (Skerra, 2000; Binz et al.,

2005). More specifically, scaffold proteins are usually much smaller in size (usually 10–20 kDa) than mAbs, consist of a single protein chain, and are often devoid of disulfide bonds, glycosylation and other post-translational modifications. Most have been engineered to be highly soluble and stable. The combination of the unique structures and biophysical properties of these molecules enable applications unique from those of mAbs, such as alternative delivery routes, targeting of intracellular proteins, simplified multi-specific formatting and robust manufacturing strategies.

One of the most well-studied classes of alternative scaffold proteins is the monobody, based upon the structure of the 10th Fibronectin type III domain (10FN3) from human fibronectin (Koide et al., 1998). Libraries of this scaffold have been engineered and selected against a multitude of research and therapeutic targets using phage display, yeast display and *in vitro* display methods (reviewed in [Jacobs and O'Neil, 2012; Koide et al., 2012b]). Originally, and in many subsequent publications, these libraries were designed as antibody mimics, randomizing the BC-, DE- and FG-loops of FN3 that are structurally analogous to antibody complementary determining regions (CDR) regions (Koide et al., 1998, 2007; Xu et al., 2002; Richards et al., 2003; Karatan et al., 2004; Parker et al., 2005; Getmanova et al., 2006; Lipovsek et al., 2007; Dineen et al., 2008; Garcia-Ibilcieta et al., 2008; Gilbreth et al., 2008; Hackel et al., 2008; Olson et al., 2008; Wojcik et al., 2010; Ramamurthy et al., 2012). Monobodies based on randomized loop libraries have even been evaluated in the clinic in recent years (Dineen et al., 2008; Bloom and Calabro, 2009). Our lab has engineered consensus FN3 domains with excellent biophysical properties and demonstrated their utility for generation of protein therapeutics (Jacobs et al., 2012). The consensus approach was undertaken as it often results in the generation molecules of exceptional stability and expression, ideal for therapeutic applications (Lehmann et al., 2000, 2002; Lehmann and Wyss, 2001; Tomschy et al., 2002; Binz et al., 2003, 2004; Forrer et al., 2004; Steipe, 2004; Midelfort and Wittrup, 2006; Dai et al., 2007; Merz et al., 2008; Jacobs et al., 2012).

It is desirable to produce scaffold libraries of various surface compositions and structures to sample larger numbers of potential epitopes on target proteins. To expand the FN3 library design beyond CDR-like loops, we analyzed a variety of naturally occurring protein–protein interactions involving FN3 domains. This structural analysis indicated that while the vast majority of the interactions involved loop residues of the natural FN3 domains, some interactions are formed by residues from the β-strands. For example, the cytokines interleukin (IL)-13 and IL-4 are bound by five FN3 domains of the IL-4 receptor and IL-13 receptor α1 (IL13Rα1) (LaPorte et al., 2008). Although the majority of the positions governing these interactions lie in the loop regions of these FN3 domains, the D-strand of IL13Rα1 is found to interact with IL-4 and IL-13 directly. Similarly, the D-strand is involved in interactions

between an FN3 domain of granulocyte colony-stimulating factor (GCSF) and the GCSF receptor, defined as 'Site II' (Aritomi *et al.*, 1999). Finally, antibodies, which have a similar topology to FN3 domains, interact with Protein A and FcRn through β-strand positions of the Vh and CH3 domains, respectively (Burmeister *et al.*, 1994; Graille *et al.*, 2000). It is thus conceivable then that the engineered FN3 domains can be randomized at strand residues to act with target molecules.

Similar to the analysis of natural FN3 domains, recent observations from X-ray crystallographic analyses of monobody/target complex structures demonstrated that the strand residues can also be important for binding, despite being held constant in the library, thus leading to the creation of a novel monobody library (Koide *et al.*, 2012a,b). This alternative design is quite different from an antibody variable domain, as the binding face incorporates both loop and non-loop residues (Wojcik *et al.*, 2010; Koide *et al.*, 2012a,b; Ramamurthy *et al.*, 2012). This library was used to successfully select monobodies against Abl SH2, GFP and hSUMO1 with affinities as high as 9 nM. Building upon this theme, we describe a new FN3 library design based upon the consensus Tenascin FN3 framework (Tencon), referring to the molecules produced from this Tencon library as 'Centyrins'. The library, which randomizes portions of the C-strand, F-strand, CD-loop and FG-loop, was panned against three targets; c-MET, murine IL-17A (mIL-17A) and rat TNFα (rTNFα), to test its utility. Specific binding molecules with an affinity as high as 21 pM were identified from the primary library. In addition, we show that Centyrins selected from this library are biologically active, have excellent biophysical properties and can be simply produced in bacteria.

## Results

### Design of the TCL14 library

The crystal structure of the consensus Tenascin FN3 domain, Tencon (PDB 3TES), was used to design a new FN3 domain library called TCL14 (Tencon Library 14). Specific residues in the C-strand, F-strand, FG-loop and CD-loop were randomized to provide a binding surface similar to that observed for FN3/Ig domain protein–protein interactions involving strand residues. For this library, the amino acid sequence of the most stable Tencon variant identified previously, Tencon25 was

used as the framework (Jacobs *et al.*, 2012). The C- and F-strands were chosen, as these two strands lie at the center of a surface of the Tencon molecule formed by the β-sheet that includes the C-, F-, D- and G-strands (Fig. 1). For the strands, three residues in each of the C- and F-strands with solvent exposed side chains were replaced with random amino acids. More specifically, these residues occur at positions 32, 34 and 36 from the C-strand and 68, 70 and 72 from the F-strand (according to numbering from PDB file 3TES). As these two β-strands lie between the FG- and CD-loops, portions of these loops were also randomized to increase the binding surface available for interacting with target molecules, including the four residues from the CD-loop nearest to the C-strand, positions 38–41 and positions 78, 79 and 81 from the FG-loop. These positions were previously shown to be tolerant of amino acid substitution (Jacobs *et al.*, 2012). Although the FG-loop is considerably longer than the CD-loop, only three positions were randomized for several reasons. First, we have found previously that inclusion of a glycine residue in the FG-loop minimizes the chance of domain swapping following library construction, a condition found to occur in some FG-loop libraries (Teplyakov *et al.*, 2013). Thus, the GG sequence of positions 76 and 77 was maintained. In addition, position S80, which falls between two positions selected for randomization, was kept as serine as this side chain is predicted to form a hydrogen bond with the backbone of the C-strand. Previous studies have shown that mutation of S80 to alanine results in a significant decrease in folding stability for Tencon (Jacobs *et al.*, 2012). Overall, the library design leads to a randomized surface including 13 positions with approximate dimensions of 30 Å in length (measured from the backbone Cα of position 78 to that of position 38) and 11 Å in width (measured from the backbone Cα of position 32 to that of position 81.

To generate the Centyrin library, the gene sequence encoding Tencon was amplified by polymerase chain reaction (PCR) to include the degenerate codon NNS in each of the abovementioned positions. This results in a theoretical distribution of all 20 amino acids ranging from 3.1 to 9.3% (Bosley and Ostermeier, 2005). In addition, a TAG stop codon is theoretically incorporated at a 3.1% frequency, resulting in a predicted rate of non-functional library members resulting from stop codons of 33.8%. A Tac promoter sequence was added to the 5′-end of the amplified library sequence by PCR and this fragment ligated to the gene sequence for RepA to implement CIS
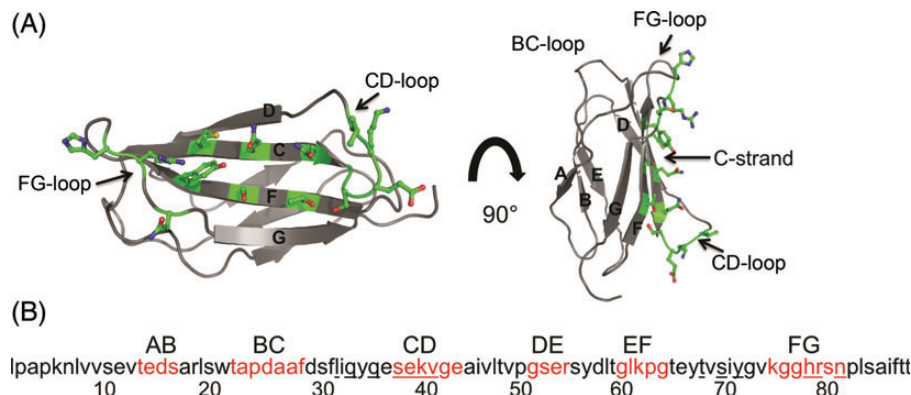
**Fig. 1.** Design of the Centyrin TCL14 library. The crystal structure of Tencon (PDB 3TES) is shown with the randomized positions of the C-strand, F-strand, CD-loop and FG-loop depicted in green (**A**). The image on the right is rotated 90° around the *z*-axis compared with that on the left. The sequence of Tencon25 is shown with loop positions in red (**B**). Library positions are underlined. The sequence is numbered below as in PDB file 3TES.

display for the isolation of binding molecules (Odegrip *et al.*, 2004). Following library construction, the Centyrin portion of the library was PCR amplified and subcloned into a pET vector for sequence analysis. From 149 readable sequences, 43% contained a stop codon, slightly higher than the expected theoretical value of 33% (Bosley and Ostermeier, 2005), leaving 56% of the library functional, full-length molecules.

### Biophysical properties of TCL14 library members

Our previous mutagenesis studies on the stability of Tencon were focused mainly on the loop positions as well as the portions of the strands directly adjacent to those loops (Jacobs *et al.*, 2012). Thus, we sought to determine how randomization of the β-strand residues in combination with randomization of portions of the FG- and CD-loops affects the biophysical properties of Centyrins. The Tencon portion of the TCL14 library was amplified by PCR and subcloned into a pET vector for expression of random library members in *Escherichia coli*. Sixty-nine clones that were determined to be full-length sequences free of stop codons were expressed in 5 ml cultures and purified by a one-step method employing high-throughput Ni-NTA chromatography. Size-exclusion chromatography (SEC) using a Superdex 75 column was used to assess the aggregation state of each purified protein. Samples were considered to be soluble and monomeric if the elution time of the sample was between 5.7 and 6.2 min, as the elution time of monomeric Tencon25 was 5.8 min on this column. A summary of the size-exclusion results is found in Table I. Seventy percent of the clones purified and eluted from the column with an elution time consistent with that of a monomeric species. This percentage is further increased to 83% when clones that contain a free cysteine, which we have found to oxidize in solution in some cases causing formation of a mixed species of monomer and dimer Centyrins, are excluded from analysis (data not shown). Only a small percentage of clones (6%) had no signal on the size-exclusion chromatogram, indicating very low or insoluble expression. The SEC results for 4% of the clones were indicative of larger aggregate formation. Examples of chromatography traces for each type of molecule described in Table I can be found in Supplementary Fig. S1.

The conformational stability of 16 monomeric library members selected at random was assessed by differential scanning calorimetry in phosphate-buffered saline (PBS). A mean melting temperature of $70.2 \pm 10.1°C$ was obtained for this set of molecules with a highest and lowest $T_m$ observed of 87.3 and 45.6°C, respectively (Supplementary Fig. S2). For comparison, a $T_m$ of 93°C was obtained for the Tencon25 consensus sequence. Overall, the size-exclusion and differential scanning calorimetry (DSC) data indicate that the randomization of the positions described in Fig. 1 is well tolerated in the Tencon scaffold.

### Selection of Centyrins that bind to target proteins

To assess the utility of this library design for producing new binding molecules, the TCL14 library was panned against three different targets, human c-MET, rTNFα and mIL-17A using CIS display (Odegrip *et al.*, 2004). Up to nine rounds of CIS display were completed for each target with increasing stringency of selection used for later rounds (see the Methods section). Following panning, screening for binders to c-MET and rTNFα was performed by enzyme-linked immunosorbent assay (ELISA) using *E.coli* lysates expressing individual Centyrins. For these targets, a secondary screen was also completed to find clones with the desired biological activity; inhibition of human growth factor (HGF) binding to recombinant c-MET or inhibition of rTNFα stimulation of HEK-Blue cells. For selections against mIL-17A, the initial ELISA binding screen was omitted due to the high hit rates obtained with other Centyrin libraries (data not shown) and the selection outputs thus screened directly for bioactivity via an assay measuring inhibition of mIL-17A/mIL-17 receptor interactions. Table II describes the hit rate, or percentage of screened clones that bound to the target protein, as well as the rate of biologically active clones obtained for each selection experiment. Specific binding was defined for each target based on background signals of each antigen. An ELISA signal of 10-fold greater than that of the signal for binding to a non-specific protein (human serum albumin) was used as the minimum requirement for counting a clone as a hit. Hit rates from 42 to 76% were obtained for the three selections with 29–68% of the sequenced hits found to be unique clones. Centyrins that could inhibit the biological activity of each target were identified in each case.

Higher affinity clones were isolated by repeating the screening assays at greater dilutions of *E.coli* lysate (up to 100 000-fold). The binding affinities of one clone from each selection that retained strong binding at the highest dilutions were determined by surface plasmon resonance (SPR; Fig. 2, Table II). Representative clones were P114-A3 for c-MET, TP1-C6 for mIL-17A and P191-22 for rTNFα. Slow off-rates were obtained for variants selected against all three targets with $K_D$ values of 400 pM, 1.19 nM and 1.8 nM, respectively, for the anti-c-MET, anti-TNFα and anti-IL17A clones when the biotinylated target protein was captured on the SPR surface

**Table I.** Summary of SEC results

|                       | All samples (%) | Exclude cysteine (%) |
|-----------------------|-----------------|----------------------|
| Monomeric             | 70              | 83                   |
| Mixture monomer/dimer | 17              | 10                   |
| Large aggregate       | 4               | 5                    |
| No signal             | 6               | 2                    |
| Late elution          | 3               | 0                    |

**Table II.** Summary of Screening and Characterization

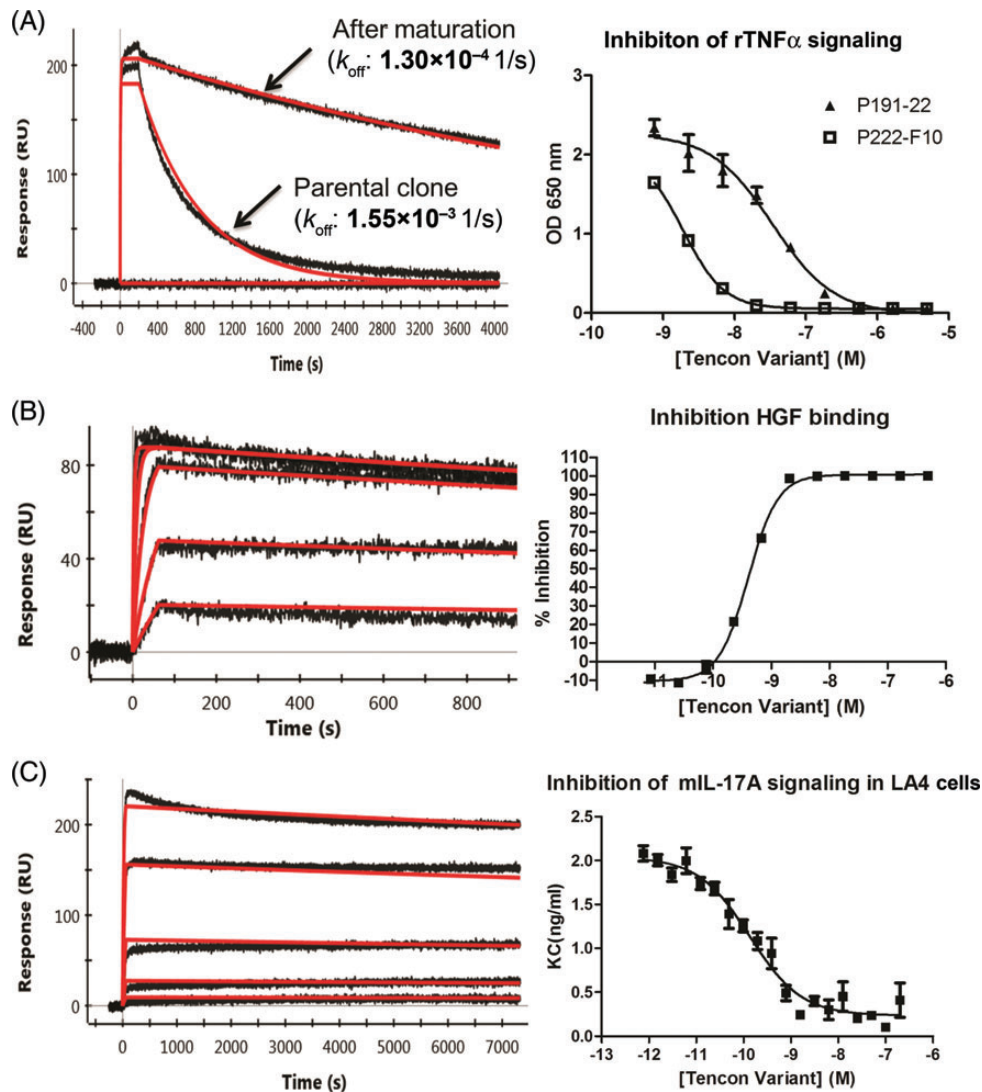|                                    | Target |  |  |
|------------------------------------|--------|--------|--------|
|                                    | Human c-MET | mIL-17A | rTNFa |
| Round screened                     | 7      | 9      | 7      |
| Clones screened                    | 352    | 160    | 88     |
| Number of binders                  | 147    | Not determined | 67 |
| Number of inhibitors               | 135    | 79     | 11     |
| Number of unique sequences         | 39     | 54     | 20     |
| $k_a$ representative clone (1/ms)   | $6.27 \times 10^5$ | $5.68 \times 10^5$ | $1.06 \times 10^6$ |
| $k_d$ representative clone (1/s)    | $2.67 \times 10^{-4}$ | $1.20 \times 10^{-5}$ | $1.27 \times 10^{-3}$ |
| $K_D$ representative clone (M)      | $4.25 \times 10^{-10}$ | $2.12 \times 10^{-11}$ | $1.19 \times 10^{-9}$ |
| $IC_{50}$ bioassay (nm)             | 0.40   | 0.071  | 33.8   |

**Fig. 2.** Binding and biological activity of selected TCL14 Centyrins. Panels on the left show binding affinity measurements by SPR while those on the right show inhibition of biological activity for rTNFα (**A**), c-MET (**B**) and mIL-17A (**C**). The corresponding values of the kinetic constants and IC$_{50}$ measurements for each molecule can be found in Table II. Sensograms are shown for both the parent and affinity matured anti-rTNFα molecules. Off-rates of $1.27 \times 10^{-3}$ and $1.29 \times 10^{-4}$ 1/s were measured, respectively.

(Fig. 2). For anti-mIL17A clone TP1C6, an affinity of 21 pM was obtained when changing the orientation of the assay such that the Centyrin was captured directly on the surface before flowing mIL-17A over the surface. This format was utilized for IL-17A as this antigen was found to be inactive during re-generation of the SPR chip surface between experiments when directly coupled. The higher affinity obtained by this method also agrees more closely with the cell-based potency data (described below). However, because of the dimeric nature of mIL-17A, we cannot rule out conclusively the contribution of avidity effects to this binding constant.

In addition to high-affinity binding, all three selected Centyrins were able to potently inhibit the biological activity of the target molecule in the respective antigen-specific assays (Fig. 2, Table II). Clone P114-A3 was shown to inhibit the interaction of HGF and recombinant c-MET with an IC$_{50}$ of 400 pM (Fig. 2B). Centyrins selected against mIL-17A were first screened for inhibition of mIL-17A binding to the murine IL-17 receptor captured on a Maxisorp plate (data not shown).

A more sensitive cell-based assay monitoring the release of KC from LA-4 cells was used to further characterize the best Centyrins. TP1C6 inhibited mIL-17A signaling in this assay with a potency of 71 ± 50 pM (averaged over three replicate experiments) (Fig. 2C). Finally, inhibition of TNFα-induced NF-κB activity in HEK-Blue TNF-α/IL-1β cells was used to assess the bioactivity of anti-rTNFα Centyrins. Clone P191-22 inhibited rTNFα signaling with an IC$_{50}$ of 33.8 nM (Fig. 2A).

### Definition of binding surfaces

Scanning mutagenesis experiments were completed to define the positions of the library that contributed most significantly to target binding for the c-MET (P114-A3), mIL-17A (TP1-C6) and rTNFa (P191-22) inhibitors. Each amino acid position derived from the TCL14 library of the TP1-C6 and P191-22 Centyrins were individually mutated to alanine and each mutant tested for activity. In the cases where the parent molecule residue was an alanine, mutation was made to serine or lysine. In addition, clone TP1-C6 contained a
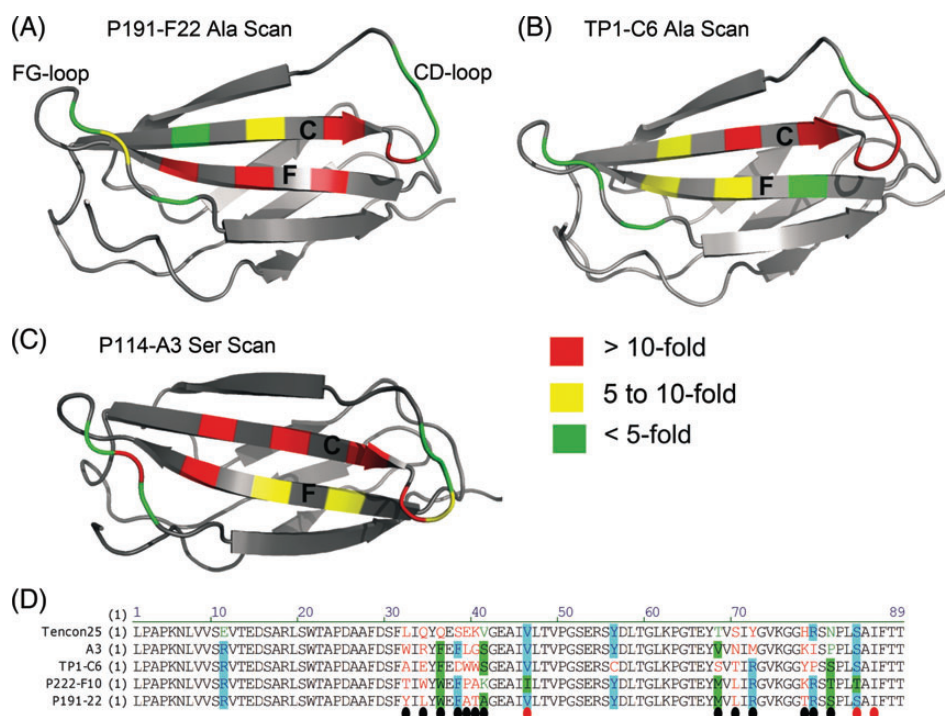
**Fig. 3.** Summary of scanning mutagenesis studies for P191-22 (**A**), TP1-C6 (**B**) and P114-A3 (**C**) molecules. The magnitude of the decrease in activity for each mutant is mapped onto the position of the Tencon crystal structure according to the color table. The exact values for activity of each mutant can be found in Supplementary Tables SI–SIII. A sequence alignment compares the sequences selected from panning against Tencon25 (**D**). Black circles beneath the alignment indicate the positions of the TCL14 library while red circles indicate additional positions randomized during affinity maturation.

cysteine incorporated into the framework by spurious mutagenesis during panning (Fig. 3D). This position was reverted to tyrosine for further analysis without an effect on activity (Supplementary Table SIII). For mIL-17A, SPR was used to assess the binding affinity of mutants while for rTNFα, functional inhibition of rTNFα stimulation of HEK-Blue cells was used to determine the effect of each mutation. For the anti-c-MET Centyrin P114-A3, the binding surface was defined in the context of a bispecific Centyrin. In this construct, P114-A3 was linked to a second Centyrin that binds to another growth factor receptor to form a bispecific molecule. Linking of P114-A3 to the second Centyrin does not affect binding to recombinant c-MET (data not shown, manuscript in preparation). For c-MET-binding Centyrins, each position derived from the library scanning mutagenesis was performed using serine rather than alanine and the effect on binding affinity determined by SPR. Position P114-A3 S41 was not mutated in this study. The detailed results from the scanning mutagenesis experiments can be found in Supplementary Tables SI–SIII. Figure 3 maps the magnitude of changes in binding affinity or activity onto the surface of the Tencon structure for each molecule with residues colored in green exhibiting <5-fold loss in activity, yellow 5–10 fold and red >10-fold. The F-strand appears to be most important for rTNFα binding by P191-22 with the last residue of the C-strand and the first residue of the CD-loop also critical for binding. Anti-mIL17A Centyrin TP1C6 shows a different pattern of activity, with residues of the CD-loop contributing most prominently to mIL-17A binding along with positions 36 and 38 of the C-strand. Finally, anti-c-MET P114-A3 is dependent upon a wider surface for c-MET binding including key residues from both the CD- (position 38) and FG- (position 79) loops as well as the entire C-strand and portions of the F-strand.

## Affinity maturation of P191-22

While panning of the TCL14 library against human c-MET and mIL-17A produced binders with subnanomolar affinity, the highest affinity achieved for rTNFa was 1.19 nM. Furthermore, the $IC_{50}$ of this clone for inhibiting rTNFa stimulation of cells was only 33 nM. Thus, the alanine scanning data for this clone were used to design an affinity maturation library to improve the potency. A new library was built in which the sequence of P191-22 was held constant at positions deemed critical for binding (i.e. W36, F38, M68, L70 and R72), while the remaining positions from the original TCL14 library design (i.e. 32, 34, 39, 40, 41, 78, 79 and 81) were re-randomized to have an equal probability of 18 amino acids (no cysteine or methionine) using Slonomics technology (Van den Brulle *et al.*, 2008). In addition, positions 46 (D-strand), 84 (F-strand) and 86 (F-strand) were also randomized to expand the potential interaction surface with the target protein. The new library was amplified and subcloned into the CIS display system and subjected to nine rounds of panning under stringent conditions. Screening was completed as above for the initial rTNFα panning. A number of clones that could bind to rTNFα by ELISA at a higher dilution of *E.coli* lysate compared with the parent molecule were identified and the binding affinity determined by SPR. Figure 2A shows the decrease in off-rate obtained for the best clone, P222-F10. An affinity of 150 pM was calculated from this analysis, representing an 8-fold increase in affinity following the maturation process. In addition, an increase in potency in the cell-based rTNFα inhibition assay from 33 to 2 nM was observed. A sequence alignment between the parent clone (P191-22) and matured clone (P222-F10) is shown in Fig. 3D. All of the randomized positions, with the exception of I86, were changed in the

matured clone compared with the parent. Interestingly, the three additional positions included from the D- and F-strands were reverted back to the amino acid from the starting Tencon25 consensus sequence.

## Discussion

Selection of high-affinity binding molecules is of great importance to the generation of therapeutic proteins. The FN3 domain has been exploited as a scaffold for isolating binding molecules in various forms over the years (Koide *et al.*, 1998, 2007, 2012a,b; Skerra, 2000; Karatan *et al.*, 2004; Parker *et al.*, 2005; Hackel *et al.*, 2008; Bloom and Calabro, 2009; Wojcik *et al.*, 2010). In this report, a new library design, TCL14, is described with the diversified region centered in the second β-sheet of the Tencon FN3 domain. In addition to these strand positions, select residues of the CD- and FG-loops are also randomized to create the binding surface. This library design differs considerably from the antibody-like BC-/DE-/FG-loop library designs traditionally used to isolate novel FN3-based molecules but is more similar to the recent 'side-and-loop' library described by Koide *et al.* (2012a,b), in which certain positions of the D- and C-strands are randomized in combination with the FG- and CD-loops. Despite some similarities, the TCL14 library differs from the 'side-and-loop' design in several ways. First, we chose to randomize the C- and F-strands that lie directly between the FG- and CD-loops in the center of the DCFG-strand (Fig. 4) in contrast to the D- and C-loops combination used previously. Further, the side-and-loop library of Koide *et al.* employed a long FG loop with diversified length of 7–13 residues while the TCL14 library randomizes only 3 residues of this loop. As such, it is expected that the TCL14 library relies significantly less on the FG-loop for target binding (see below). In order for any new library to be successfully used for engineering target binding, it is requisite that the mutations in selected positions maintain a certain degree of conformational stability. As both the Tencon and 10FN3 scaffolds are highly stable proteins (Koide *et al.*, 1998; Clarke *et al.*, 1999; Cota and Clarke, 2000; Jacobs *et al.*, 2012), we speculate that the TCL14 design can be successfully applied to the 10FN3 scaffold and the side-and-loop design applied to the Tencon scaffold. However, careful measurements of stability will be needed to confirm that the two different FN3 scaffold can tolerate substitutions at the same positions.

Besides the location of diversified residues, an additional difference between these library designs is the amino acid distribution employed. A complex distribution of amino acids was applied in the case of the side-and-loop library, in which proline and glycine were excluded from the C-strand and only Ala, Glu, Lys and Thr incorporated into the D-strand positions to improve stability and discourage aggregation (Koide *et al.*, 2012a,b). In contrast, the TCL14 library described here relies exclusively on a simple NNS codon that incorporates a mixture of codons for all 20 amino acids. Despite this simple design, it is demonstrated here that Centyrins selected from TCL14 are highly stable and soluble (Supplementary Figs. S1 and S2). For example, the anti-c-MET clone P114-A3 described in this report was found to have a melting temperature of 87°C and affinity of 400 pM (data not shown).

Despite using NNS randomization at only 13 positions, Centyrins with remarkable affinity against several targets were readily selected. For two targets, c-MET and mIL-17A, Centyrins with affinities of 400 and 21 pM were isolated after nine rounds of CIS display selections (Fig 2, Table II). One potential explanation for the high affinities of selected Centyrins is that for binding through strand positions there is less conformational flexibility and thus less entropic cost upon target binding. Especially for larger loop libraries, the entropic considerations may play an important role in limiting the affinity of selected binders. Of note, the high affinities achieved in binding these targets were obtained after panning only the primary library as no affinity maturation step was needed. Other studies of 10FN3 libraries have also produced binding molecules of such high affinity (Hackel *et al.*, 2008); however, a more complicated maturation scheme involving random mutagenesis, loop shuffling and yeast display was used to generate these molecules. Indeed, comparisons to FN3 libraries constructed in various other labs are rendered difficult as those libraries are ultimately built on a different FN3 scaffold (the 10th FN3 domain from human fibronectin) and utilize different selection systems like phage display and yeast display (Koide *et al.*, 1998, 2007, 2012a,b; Skerra, 2000; Karatan *et al.*, 2004; Parker *et al.*, 2005; Hackel *et al.*, 2008; Bloom and
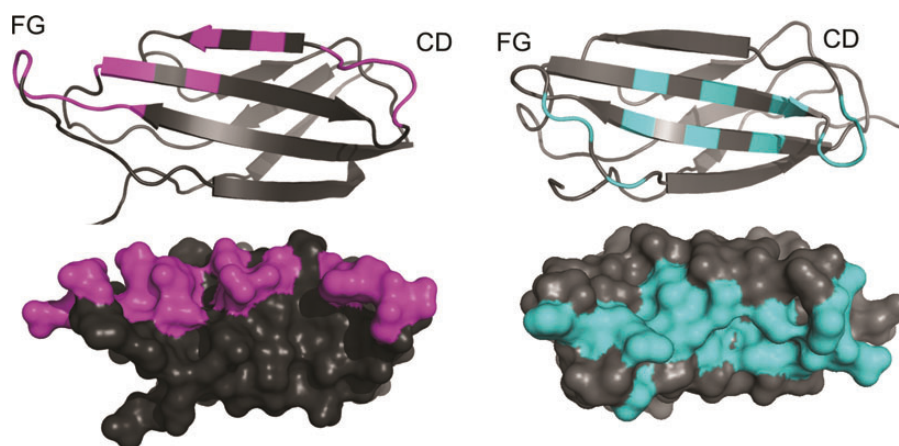
**Fig. 4.** Comparison of the side-and-loop library design to TCL14. The positions randomized in the side-and-loop library (**A**) are depicted in purple while those randomized in the TCL14 library are depicted in cyan (**B**).

Calabro, 2009; Wojcik *et al.*, 2010). Nevertheless, the results presented in this study confirm the utility of TCL14 in combination with CIS display to produce high affinity, stable Centyrins against multiple target proteins in rapid fashion.

In contrast to the results for c-MET and mIL-17A, Centyrins of only moderate affinity (1.9 nM) were selected against rTNFα using the primary TCL14 library. In this case, a simple affinity maturation strategy was designed based on the results of alanine scanning mutagenesis studies. A resulting maturation library, in which the key rTNFα interaction positions were held constant was then used to select a new Tencon variant with an improved affinity of 150 pM. During this maturation step, several residues from the D- and G-strands were added to those diversified in an attempt to increase the size of the binding surface. Interestingly, all three of these positions were reverted to the sequence of the most stable Tencon framework, perhaps due to a selective pressure for these amino acids to stabilize the FN3 fold. Indeed, two of these positions were previously identified to contribute significantly to Tencon stabilization (Jacobs *et al.*, 2012).

Of critical importance to the iterative design of new scaffold libraries is a molecular understanding of the binding interface formed between the scaffold and the target antigen. Despite a lack of high-resolution structural data describing complexes of the Centyrins bound to the respective target proteins, we have been able to map the key TCL14 positions responsible for binding by scanning mutagenesis. Interestingly, the Centyrins selected against c-MET, mIL-17A and rTNFα show different patterns in these studies (Fig 3). In all three cases, some portion of the strand residues were determined to be critical for activity but the exact strand positions and magnitude of importance differ among the members of the set. Likewise, differences in the importance of loop residues are also clear. TP1-C6, the mIL-17A binder, was found to be mostly dependent upon the CD-loop for binding whereas P114-A3 relied on key residues in both the FG- and CD-loops for c-MET interactions. Future structural determinations of Centyrins bound to target proteins will further elucidate key interactions formed from this scaffold.

An important driver for the creation of new binding interfaces on scaffold proteins is the hypothesis that alternative designs may lead to alternative epitopes recognized on target proteins. Koide *et al.* (2012a,b) hypothesize that the concave shape of strand–loop libraries may be more amenable to binding flatter, concave protein–protein interaction surfaces while extended loop libraries may be more successful at reaching into grooves or clefts of target proteins. In addition, recent work from Skerra and colleagues suggests that an immunoglobulin variable domain can be engineered to have high affinity for a novel Huntington epitope where the binding interface is dominated by β-sheet residues. The authors postulate that such non-canonical modes of binding may occur more widely than originally thought and suggest that targeted engineering of the β-sheet region may be an alternative strategy to generate Ig domain binders (Schiefner *et al.*, 2011). We share enthusiasm for these hypotheses and have now completed selections against ∼30 different targets with Centyrin loop libraries and the TCL14 library. A detailed comparison between the results obtained for these experiments is beyond the scope of this manuscript but our results suggest that in some cases different epitopes are indeed recognized preferentially by these different Centyrin library designs. Future publications will attempt to dissect these results in more detail.

## Methods

### Antigen sources

Recombinant mIL-17 receptor-Fc, recombinant Human HGF and recombinant c-MET-Fc were purchased from R&D Systems (Minneapolis, MN, USA). mIL-17A was produced in house from HEK cells. Mouse TNF Receptor 2 was purchased from Sino Biological Inc. (Beijing, China). A single-chain version of rTNFα was designed according to that previously described for human TNFα (Krippner-Heidenreich *et al.*, 2008). This construct was expressed in strain BL21 *E.coli* and purified by Ni-NTA chromatography and SEC.

### Library construction

To randomize non-contiguous stretches of Tencon25 described in the TCL14 library design, the Tencon25 gene, including an E11R point mutation, was randomized at positions L32, Q34, Q36 (C-strand), S38, E39, K40, V41 (CD-loop), T68, S70, Y72 (F-strand), H78, R79 and N81 (FG-loop) using the PCR. Briefly, two DNA cassettes, the first incorporating degenerate nucleotides in the C-strand and C:D loop and the second incorporating degenerate nucleotides in the F-strand and F:G loop were generated by PCR. Following the creation of each cassette, the two cassettes were combined by restriction digest, amplified by PCR and finally appended to the gene encoding for RepA for CIS display (Odegrip *et al.*, 2004). The C-C:D cassette was made using primer CD 5′ Long (GCGCGTCT GTCTTGGACCGCGCCGGACGCGGCGTTCGACTCTTTC) as the forward primer, GC-FG 5′ Long N46V (GTATTCGGTA CCCGGTTTCAGACCGGTCAGGTCGTAAGAACGTTCAG AACCCGGAACGGTCAGAACGATCGCTTCACC) as the reverse primer and Tencon C-CD N46V (GCGGCGTTCGAC TCTTTCNNSATCNNSTACNNSGAANNSNNSNNSNNSGG TGAAGCGATCGGTCTGACCGTTCCGGGTTCTGAACGTT CTTACGACCTGACCGGTCTGAAACCGGGTACCGAATAC) with degenerate positions as the template. For the F-F:G cassette, FG 5′ Long N46V (GGTGAAGCGATCGTTCTGACCGTTCC GGGTTCTGAACGTTCTTACGACCTGACCGGTCTGAAAC CGGGTACCGAATAC) was used as the forward primer, FG 3′ (GGTGGTGAAGATCGCAGACAG) as the reverse primer and Tencon F-FG-Sf E86I-R with degenerate positions (GGTGG TGAAGATCGCAGACAGCGGSNNAGASNNSNNACCACC TTTAACACCSNNGATSNNAACSNNGTATTCGGTACCCG GTTTCAGACCGGTCAGGTCGTA) as the template for the F-F:G cassette. BsaI restriction sites were added to the cassettes by PCR using primers CD 5′ BsaI (AAAGGTCTCGCG TCTGTCTTGGACCGCG) as the forward primer and CD 3′ BsaI (AAAGGTCTCAACGATCGCTTCACCAAC) as the reverse primer for the C-C:D cassette and FG 5′ BsaI (AAA GGTCTCATCGTTCTGACCGTTCCG) as the forward primer and C-SDG28a (SEQ Id No. 13) as the reverse primer for the F-F:G cassette. The TAC promoter region was amplified with a fragment of the 5′-end of Tencon and a 3′ BsaI restriction site using primers R1RecFor (GAACGCGGCTACAATTAA TACATAACC) as the forward primer and TAC-Tencon Reverse BsaI (AAAGGTCTCAGACGCGCAGAGTCTTC) as the reverse primer. The full-length library was constructed by digesting the three cassettes with BsaI restriction enzyme (NEB, Ipswich, MA, USA) and performing a triple ligation using T4 DNA Ligase (NEB). The full-length ligation product was digested with NotI restriction enzyme (NEB) and a digestion and ligation reaction was performed with RepA in the

presence of NotI and PspOMI (NEB). The full-length TAC-TCL14-RepA CIS display library was amplified by PCR from the digestion/ligation reaction using R1RecFor and DigLigRev (CATGATTACGCCAAGCTCAGAA) as the forward and reverse primers, respectively.

## Small-scale purification

To enable further characterization of either library members or selection outputs, small-scale plate-based purifications were performed. Library members/selection outputs were amplified by PCR using TCON6 (AAGAAGGAGAACCGGTATGC TGCCGGCGCCGAAAAAC) as the forward primer and TCON5 E86I short (GAGCCGCCGCCACCGGTTTAATGGTGATGGT GATGGTGACCACCGGTGGTGAAGATCGCAGACAG) as the reverse primer and subcloned by annealing into a pET15 vector modified to contain a ligase independent cloning site (pET15-LIC). The annealing reaction was transformed into BL21-Gold(DE3) *E.coli* (Agilent, Santa Clara, CA, USA) and plated for individual colonies. Single clones were picked and grown to saturation in 1 ml Luria Broth (LB) supplemented with 100 μg/ml ampicillin (LB-Amp media) in 96 deep well plates at 37°C. The following day, 25 μl was transferred to fresh 5 ml LB-Amp media in 24 deep well plates and grown at 37°C for 2 h. Isopropyl β-D-1-thiogalactopyranoside (IPTG) was added at 1 mM final concentration and protein expression was induced at 30°C for 16 h. The cells were harvested by centrifugation and subsequently lysed with Bugbuster HT (EMD Chemicals, Gibbstown, NJ, USA) supplemented with 0.2 mg/ml final chicken egg white lysozyme (Sigma-Aldrich, St Louis, MO, USA). The bacterial lysates were clarified by centrifugation and the supernatants transferred to new 96 deep well plates. The his-tagged Centyrins were purified using a 96-well Ni-NTA Multitrap Plate following the manufacturers recommendation (GE Life Sciences, Piscataway, NJ, USA).

## Analytical SEC

Purified proteins were subjected to SEC to determine the aggregation propensity of individual library members. The elution profiles of select clones were determined by injecting 10 μl of the purified proteins onto a Superdex 75 5/150 column using an Agilent 1200 HPLC with absorbance read at 280 and 214 nm. The flow rate was 0.3 ml/min with PBS as the running buffer.

## Thermal stability

DSC was used to measure thermal stability. DSC data were obtained by heating 0.5 mg/ml solutions for each clone in PBS from 35 to 95°C at a rate of 1°C/min in a VP-DSC capillary cell microcalorimeter (MicroCal, LLC, Piscataway, NJ, USA). Melting temperatures were calculated for each clone using CpCalc (MicroCal, LLC) software.

## CIS display selections

TCL14 library members that could bind specific targets were identified through several iterative rounds of selection using CIS display. Purified soluble target proteins (mIL17A, rTNFα and c-MET) were first biotinylated using the EZ-Link No-Weigh Sulfo-NHS-LC-Biotin Microtubes (Thermo Fisher, Rockford, IL, USA) followed by extensive dialysis into PBS as per the manufacturer's recommendations. For selections, 3 μg of TCL14 library DNA was *in vitro* transcribed and translated in *E.coli* S30 Linear Extract (Promega, Madison, WI,

USA) followed by blocking with CIS Block (2% bovine serum albumin (BSA)) (Sigma-Aldrich), 100 μg/ml Herring Sperm DNA (Promega), 1 mg/ml heparin (Sigma-Aldrich) and addition of biotinylated target protein at concentrations of 400 nM (Round 1), 200 nM (Rounds 2 and 3) and 100 nM (Rounds 4 and 5). For selection against rTNFα, an additional selection scheme was performed with mouse TNFR2 pre-mixed with single-chain rTNFα in a 1 : 1 molar ratio before beginning the selection. Bound library members were recovered using Neutravidin magnetic beads (Thermo Fisher) (Rounds 1, 3 and 5) or streptavidin magnetic beads (Promega) (Rounds 2 and 4) and unbound library members were removed by washing the beads 5–14 times with 500 μl PBST followed by two washes with 500 μl PBS. Finally, bound library members were eluted from the beads by incubating with $1\times$ Pfx amplification buffer (Invitrogen, Carlsbad, CA, USA) heated to 75°C. PCR was used to amplify the Centyrins and the resulting product was digested with NotI and ligated to a PspOMI-digested RepA DNA fragment. Finally, the resultant full-length product was amplified by PCR to enable the next round of selection.

## Selection for higher affinity

Outputs from Round 5 were prepared as described above and subjected to additional iterative rounds of selection with the following changes to push for faster on-rates and slower off-rates: incubation of biotinylated target antigen was decreased from 1 h to 15 min and bead capture was decreased from 20 to 15 min, biotinylated antigen was decreased to 25 nM (Rounds 6 and 7) or 2.5 nM (Rounds 8 and 9), and an additional 1 h wash was performed in the presence of an excess of non-biotinylated target antigen.

## Lysate generation for screening

Outputs from Rounds 5 and 9 of panning were amplified by PCR using primers and subcloned by annealing into a pET15 vector incorporating a ligase independent cloning site. The annealing reaction was transformed into BL21-Gold(DE3) *E.coli* (Agilent) and plated for individual colonies. Single clones were picked and grown to saturation in 1 ml LB with ampicillin in 96 deep well plates at 37°C. The following day, 25 μl was transferred to fresh 1 ml LB/ampicillin media in 96 deep well plates and grown at 37°C for 2 h. IPTG was added at 1 mM final concentration and protein expression was induced at 30°C for 16 h. The cells were harvested by centrifugation and subsequently lysed with Bugbuster HT (EMD Chemicals) supplemented with 0.2 mg/ml chicken egg white lysozyme (Sigma-Aldrich). The bacterial lysates were clarified by centrifugation and the supernatants were transferred to new 96 deep well plates and tested for binding to the target protein by ELISA.

## Binding ELISA

ELISA was performed on individual clones from select panning outputs to determine if the selections produced target-specific binders. Maxisorp plates (Nunc, Rochester, NY, USA) were coated with 0.1 μg anti-His antibody (Qiagen, Valencia, CA, USA) overnight, washed with Tris-buffered saline, pH 7.4 with 0.05% Tween-20 (TBST) and blocked using StartingBlock T20 (Thermo Fisher). Clarified lysate was diluted in starting block 1 : 5 and the HIS-tagged proteins were captured by the anti-HIS antibody. The plates were washed with TBST and biotinylated target protein or human serum albumin,

as the control, were added at a concentration of 1 µg/ml. The plates were incubated for 1 h, washed with TBST and the biotinylated protein detected with streptavidin-HRP (Jackson ImmunoResearch, West Grove, PA, USA) and POD chemiluminescent substrate (Roche, Indianapolis, IN, USA). Binders specific for target protein were defined as having 10-fold luminescence signal above the albumin control signal and hit rate defined as the number of binders divided by the total number of clones screened.

## Affinity measurements

Affinity measurements were made by SPR methods using a Proteon Instrument (Biorad). For anti-c-MET Centyrins, goat anti-human Fc IgG (R&D systems) was directly immobilized via amine coupling (at pH 5.0) at 5 µg/ml on all six ligand channels in horizontal orientation on GLC Sensor Chip (Bio-Rad, catalog no. 176-5011) with a flow rate of 30 µl/min in PBS containing 0.005% Tween-20. The immobilization densities averaged ~1500 Response Units (RU) with <5% variation among different channels. c-MET-Fc was captured on the anti-human Fc IgG surface to a density around 600 RU in vertical ligand orientation. Selected c-MET-binding Centyrins were tested at 1 µM concentration in 3-fold dilution series of five concentrations in the horizontal orientation. A buffer blank was also injected as a sixth sample to monitor the baseline stability. The dissociation phase for all concentrations of each c-MET-binding Centyrins was monitored at a flow rate of 100 µl/min for 30 min (for those with $k_{off} \sim 10^{-2}$ s$^{-1}$ from off-rate screening), or 1 h (for those with $k_{off} \sim 10^{-3}$ s$^{-1}$ or slower). The binding surface was regenerated for the next interaction cycle using an 18 s pulse of 0.8% phosphoric acid to remove the c-MET-Fc and the bound Centyrins. The raw data were processed by subtracting two sets of reference data from the response data: (i) the interspot signals to correct for the non-specific interactions between the c-MET-binding Centyrins and the immobilized IgG surface; (ii) the buffer blank injection signals to correct for baseline drifting due to the dissociation of captured c-MET-Fc ligand surface over time. The processed data at all concentrations for each Centyrins were globally fit to a 1 : 1 simple Langmuir binding model to extract estimates of the kinetic ($k_{on}$, $k_{off}$) and affinity ($K_D$) constants.

The binding affinity of Centyrins P222-F10 and P191-22 for biotinylated rTNFα was determined using a streptavidin-coated GLC Sensor Chip. The running buffer consisted of PBS with 0.005% Tween 20 (Calbiochem, catalog no. 655204). Streptavidin (Jackson ImmunoResearch, catalog no. 016-000-084) was immobilized at 7.5 µg/ml in 10 mM acetate buffer, pH 5.0 on the chip at ~2300 RU via direct amine coupling. rTNFα (prepared at 0.1 µg/ml in running buffer) was indirectly immobilized on streptavidin-coated channels at densities ranging from 75 to 101 RU using a flow rate of 30 µl/min. Due to observed inactivation of immobilized rTNFα following exposure to 0.85% phosphoric acid for surface regeneration, rTNFα was captured on a separate ligand channel prior to each new Centyrin analysis. Each Centyrin was analyzed by injection of a concentration series ( prepared in running buffer at starting concentrations of 100 or 300 nM and serially diluted 1 : 2) in analyte channels orthogonal to the rTNFα channel. Centyrins were injected at 200 µl/min for 120 s with dissociation times of 1–2 h. One analyte channel was reserved for a running buffer blank injection to enable the

monitoring of the ligand surface over time. Raw kinetic data were subjected to double referencing (Interspot and blank analyte channel subtraction) prior to processing by Langmuir 1 : 1 global fit for the determination of affinity and kinetic rate constants. Non-specific interactions were monitored at ligand and streptavidin-free interspots as well as at ligand-free streptavidin-coated channels. Additional analyses were performed to assess for ligand density and mass transfer effects, by varying levels of immobilized rTNFα and analyte flow rates.

For Centyrin/mIL-17A affinity measurements, purified Centyrins were directly immobilized on the chip via amine coupling with varying densities (100–300 RU) at pH 5.0 and a flow rate of 30 µl/min for 5 min. Binding was determined for a 3-fold concentration dilution series of mIL-17A, starting at 100 nM. The dissociation phases for all concentrations of all samples were monitored for 1–2 h at a flow rate of 100 µl/min depending on their off-rate. A buffer sample was injected to monitor the baseline stability and the surface was not regenerated for further use. In another format, biotinylated mIL17A was directly immobilized as the ligand on a streptavidin-coated GLC Sensor Chip. Streptavidin (Jackson ImmunoResearch, catalog no. 016-000-084) was immobilized at 7.5 µg/ml in 10 mM acetate buffer, pH 5.0 on the chip at ~1900 RU via standard amine coupling in vertical orientation at a flow rate of 30 µl/min. Biotin-mIL17A ( prepared at 0.5, 0.25 µg/ml in running buffer) was then captured on streptavidin-coated channels at densities ranging from 39 to 206 RU using a flow rate of 30 µl/min. Binding of anti-mIL17A Centyrin to immobilized bt-mIL17A was tested by flowing five different concentrations of Centyrin (prepared at 2 µM starting concentration in PBST serially diluted in a 3-fold concentration series) as analytes simultaneously over the immobilized mIL17A surfaces in horizontal orientation. A sixth sample (buffer only) was injected to monitor the baseline stability. The dissociation phases for all concentrations were monitored for 15 min at a flow rate of 100 µl/min. The surfaces were regenerated using one short pulse (18 µl) of 0.8% phosphoric acid for next interaction cycle. The raw binding data were subject to double referencing by subtracting: (i) the interspot signals to correct for the non-specific interactions between analytes (Centyrins or mIL17 in different format) and the chip surface; (ii) the sixth buffer channel signals to correct for baseline drifting. The processed data were globally fit to a simple 1 : 1 Langmuir binding model without mass transport (ProteOn Manger version 3.1.0).

## Centyrin mIL17A:mIL17A receptor inhibition assay

Centyrin lysates were screened for their ability to inhibit the mIL17A:mIL17A receptor interaction. Maxisorp plates were coated with 0.2 µg/ml mIL17A Receptor Fc fusion overnight, washed with PBS, pH 7.4 with 0.05% Tween-20 (PBST) and blocked with 2% BSA, 5% sucrose in PBS. Centyrin lysates were diluted 1 : 5 in blocking solution and then mixed 1 : 1 with 20 ng/ml biotin-mIL17A. The mixture was allowed to incubate with gentle mixing for 20 min. The blocked plates were washed and 100 µl of the Centyrin lysate/biotin-mIL17A incubations were transferred and allowed to incubate for an additional hour. The plates were washed with PBST and the biotinylated protein detected with streptavidin-HRP (Jackson ImmunoResearch) and OPD colorimetric substrate (Sigma-Aldrich). Plates were read at absorbance 490 nm using an M5

plate reader (Molecular Devices). Percent inhibition for mIL-17A:mIL-17A receptor binding was defined as $100 -$ (sample/negative control $\times 100$). Percent inhibition values of 50% or greater were considered hits.

In the effort to show that the anti-mIL17A Centyrins could inhibit recombinant mIL-17A from binding to the IL-17R in its native confirmation, an LA-4 cell-based assay was employed. LA-4 cells are an epithelial cell line that was derived from mouse lung adenoma. This cell line was purchased from ATCC, and all cells used for the characterization of anti-mIL17A Centyrins were derived from the same lot, to help control lot-to-lot variability. When LA-4 cells are stimulated with IL-17, they produce a dose-dependent release of mouse KC, the ortholog to human IL-8, which is measured in the cell supernatants using a plate-based ELISA. The assay was performed by seeding $2.0 \times 10^5$ LA-4 cells per well in a $100 \, \mu l$ of culture media (Hams F12K supplemented with 2 mM L-glutamine, and 15% heat inactivated fetal bovine serum) in a 96-well tissue culture treated plate. Plates were placed in a tissue culture incubator ($37^\circ C$, 5% $CO_2$, humidified) overnight to allow cells to equilibrate. On Day 2, LA-4 cells were serum starved with Ham's F12K media containing 2 mM L-glutamine and 0.1% heat inactivated fetal bovine serum for 24 h. The cells were treated on Day 3 with a constant concentration of mIL-17A and human TNF$\alpha$, along with, TP1K-C6 at a starting concentration of 200 nM and 1 : 3 serial dilutions for 19 points. The plates were incubated for 24 h at $37^\circ C$ and 5% $CO_2$. Supernatants were harvested and stored at $-80^\circ C$ for further analysis. Mouse KC Duo Set ELISA kit (R&D Systems) was used to quantify the amount of mouse KC in the samples using the manufacturer's protocol and a 1 : 5 dilution of the samples. Raw data were then entered into the Graphpad PRISM statistics software, where it was transformed and plotted on a sigmoidal dose response curve to determine the $IC_{50}$.

## Centyrin:HGF competition assay

Centyrins lysates were screened for their ability to inhibit HGF binding to c-MET in a biochemical format. Recombinant human c-MET Fc chimera (R&D Systems, cat# 358-MT) was diluted to 0.5 $\mu g/ml$ in PBS were coated on 96-well White Maxisorp Plates (Nunc) in $100 \, \mu l$ per well. Plates were covered with a plate sealing film (VWR) and incubated overnight at $4^\circ C$. The plates were washed $2\times$ with $300 \, \mu l$ per well of Tris-buffered saline with 0.05% Tween 20 (TBS-T) (Sigma-Aldrich) on a Biotek plate washer. Assay plates were blocked with $200 \, \mu l$ per well of StartingBlock T20 (Pierce) for 1 h at room temperature with shaking and again washed $2\times$ with $300 \, \mu l$ of TBS-T. Lysates diluted in StartingBlock T20 were incubated at $50 \, \mu l$ per well on assay plates for 1 h at room temperature with shaking. Dilutions ranged from 1 : 10 to 1 : 100 000 and were performed on the Hamilton STARplus robotics system. Control wells were incubated with wild-type Centyrin in lysate at same dilution as test samples. Without washing the plates, $50 \, \mu l$ per well of biotinylated HGF (R&D Systems, cat. 294-HGN/CF, biotinylated in-house) diluted to 1 $\mu g/ml$ in StartingBlock T20 was added to the plate for a final concentration of 500 ng/ml. Control wells received either $50 \, \mu l$ per well of StartingBlock T20 or $50 \, \mu l$ per well of the diluted HGF. The plates were incubated for 30 min at room temperature with shaking. Plates were then washed four times with $300 \, \mu l$ per well of TBST and incubated with $100 \, \mu l$ per

well of streptavidin-HRP (Jackson ImmunoResearch) at a 1 : 2000 dilution in TBST for 30–40 min at room temperature with shaking. Again the plates were washed four times with $300 \, \mu l$ per well of TBST. To develop signal, $50 \, \mu l$ per well of POD Chemiluminescence Substrate (Roche), prepared according to manufacturer's instructions, was added to the plate and within $\sim 3$ min read on the Molecular Devices M5 using SoftMax Pro. Luminescence was read from the top with an integration time of 500 ms and an output reading of raw fluorescence units (RFU). Percent inhibition was determined using the following calculation: $100 - ((RFU_{sample} - mean RFU_{No \, bt-HGF \, control})/(mean RFU_{bt-HGF \, control} - mean RFU_{No \, bt-HGF \, control}) \times 100)$. Percent inhibition values of 50% or greater were considered hits. A dose response curve for P114-A3 was generated with starting concentrations of 5 $\mu M$ and below and then tested in the assay format above. The data were plotted as percent inhibition against the logarithm of Centyrin molar concentrations and $IC_{50}$ values were determined by fitting data to a sigmoidal dose response with variable slope using GraphPad Prism 4.

## Inhibition of rTNF$\alpha$ activity

HEK-Blue$^{TM}$ TNF-$\alpha$/IL-1$\beta$ cells (Invivogen, San Diego, CA, USA) were maintained in assay media (DMEM + glucose supplemented with 10% HIFBS, 50 U/ml penicillin, 50 $\mu g/ml$ streptomycin, 100 $\mu g/ml$ Normocin and 100 $\mu g/ml$ Zeocin) at $37^\circ C$, 5% $CO_2$. Dose response curves of rTNF$\alpha$ were prepared in assay media (ranging from 0 to 10 nM; 1 : 3 dilutions). HEK-Blue$^{TM}$ TNF-$\alpha$/IL-1$\beta$ cells were manually detached from culture flask, placed in a 50 ml conical tube and spun at 1200 rpm for 5 min in a Thermo Scientific Megafuge 40R. Cells were counted and adjusted to a concentration of $5.0 \times 10^5$/ml in assay media. Hundred microliters of dose response curve was added to a clear 96-well tissue culture plate followed by $100 \, \mu l$ of cell suspension. The plates were incubated at $37^\circ C$, 5% $CO_2$ overnight. The following day, $20 \, \mu l$ of each cell supernatant was mixed with $180 \, \mu l$ of Quanti-Blue$^{TM}$ (Invivogen) in a clear 96-well plate to measure secreted embryonic alkaline phosphatase. The plate was incubated for 40 min at $37^\circ C$ and absorbance at 650 nm was read. Absorbance data were plotted as a function of rTNF$\alpha$ concentration to a sigmoidal dose response with variable Hill Slope using the PRISM software (GraphPad PRISM) to determine $EC_{50}$ value.

Dose response curves of small-scale purified Centyrins were prepared in assay media (ranging from 0 to 10 $\mu M$; 1 : 3 dilutions). HEK-Blue$^{TM}$ TNF$\alpha$/IL-1$\beta$ cells were manually detached from culture flask, placed in a 50 ml conical tube and spun at 1200 rpm for 5 min in a Thermo Scientific Megafuge 40R. Cells were counted and adjusted to a concentration of $5.0 \times 10^5$/ml in assay media. Fifty microliters of each dose response curve followed by 50 $\mu l$ rTNF$\alpha$ (30 pM, final concentration) and $100 \, \mu l$ of cell suspension were added to a clear 96-well tissue culture plate. The plates were incubated at $37^\circ C$, 5% $CO_2$ overnight. The following day, $20 \, \mu l$ of each cell supernatant was mixed with $180 \, \mu l$ of Quanti-Blue$^{TM}$ (Invivogen) in a clear 96-well plate to measure secreted embryonic alkaline phosphatase. The plate was incubated for 40 min at $37^\circ C$ and absorbance at 650 nm was read. Absorbance data were plotted as a function of Centyrin concentration to a sigmoidal dose response with variable Hill

Slope using the PRISM software (GraphPad PRISM) to determine $IC_{50}$ values.

## Protein expression and purification

Gene sequences encoding Centyrin mutants or single-chain rTNFα were produced by DNA2.0 and subcloned into pJexpress401 vector for expression via the T5 promoter. The resulting plasmids were transformed into *E.coli* BL21 Gold (Stratagene) for expression. A single colony was picked and grown in LB supplemented with kanamycin and incubated 18 h at 37°C. One liter Terrific Broth, supplemented with kanamycin, was inoculated from these subcultures and grown at 37°C for 4 h while shaking. Protein expression was induced with 1 mM IPTG, once the optical density at the absorption of 600 nm reached 1.0. The protein was expressed for 18 h at 30°C. Cell paste was harvested by centrifugation at 6000 *g* and stored at −20°C until purification.

The frozen cell pellet (∼25 g) was thawed for 30 min at room temperature and suspended in 125 ml of BugBuster protein extraction reagent supplemented with 0.2 mg/ml recombinant lysozyme and incubated for 1 h on a shaker. The lysate was clarified by centrifugation at 74 600 *g* for 25 min. The supernatant was applied onto 5 ml Qiagen Ni-NTA cartridge immersed in ice, using an AKTA AVANT chromatography system. The Ni-NTA column was equilibrated in 25.0 ml of 50 mM Tris-HCl buffer, pH = 7.0 containing 0.5 M NaCl and 10 mM imidazole (Buffer A) at a flow rate of 5 ml/min. The protein was bound to the Ni-NTA column by sample pump flowing at 4 ml/min. After binding the protein to the column, the column was washed with 100 ml of 50 mM Tris-HCl buffer, pH7.0 containing 0.5 M NaCl and 10 mM imidazole (Buffer A), with 100 ml of 50 mM Tris-HCl buffer, pH7.0 containing 0.5 M NaCl, 10 mM imidazole, 1% CHAPS detergent and 1% *n*-octyl-β-D-glucopyranoside (Buffer A2), and 100 ml of 50 mM Tris-HCl buffer, pH7.0 containing 0.5 M NaCl and 10 mM imidazole (Buffer A). The protein was eluted with 8 ml of Buffer A supplemented with 250 mM imidazole (Buffer B), and the single elution fraction used for preparative gel-filtration on a TSK Gel G3000SW 21.5 × 600 mm$^2$ column (Tosoh) at room temperature in PBS pH 7.4 at flow rate 10 ml/min using an AKTA-AVANT chromatography system.

## Supplementary data

Supplementary data are available at *PEDS* online.

## Acknowledgments

## References

Aritomi,M., Kunishima,N., Okamoto,T., Kuroki,R., Ota,Y. and Morikawa,K. (1999) *Nature*, **401**, 713–717.

Binz,H.K., Stumpp,M.T., Forrer,P., Amstutz,P. and Pluckthun,A. (2003) *J. Mol. Biol.*, **332**, 489–503.

Binz,H.K., Amstutz,P., Kohl,A., Stumpp,M.T., Briand,C., Forrer,P., Grutter,M.G. and Pluckthun,A. (2004) *Nat. Biotechnol.*, **22**, 575–582.

Binz,H.K., Amstutz,P. and Pluckthun,A. (2005) *Nat. Biotechnol.*, **23**, 1257–1268.

Bloom,L. and Calabro,V. (2009) *Drug Discov. Today*, **14**, 949–955.

Bosley,A.D. and Ostermeier,M. (2005) *Biomol. Eng.*, **22**, 57–61.

Burmeister,W.P., Huber,A.H. and Bjorkman,P.J. (1994) *Nature*, **372**, 379–383.

Clarke,J., Cota,E., Fowler,S.B. and Hamill,S.J. (1999) *Structure*, **7**, 1145–1153.

Cota,E. and Clarke,J. (2000) *Protein Sci.*, **9**, 112–120.

Dai,M., Fisher,H.E., Temirov,J., Kiss,C., Phipps,M.E., Pavlik,P., Werner,J.H. and Bradbury,A.R. (2007) *Protein Eng. Des. Sel.*, **20**, 69–79.

Dineen,S.P., Sullivan,L.A., Beck,A.W., Miller,A.F., Carbon,J.G., Mamluk,R., Wong,H. and Brekken,R.A. (2008) *BMC Cancer*, **8**, 352.

Forrer,P., Binz,H.K., Stumpp,M.T. and Pluckthun,A. (2004) *Chembiochem*, **5**, 183–189.

Garcia-Ibilcieta,D., Bokov,M., Cherkasov,V., Sveshnikov,P. and Hanson,S.F. (2008) *Biotechniques*, **44**, 559–562.

Getmanova,E.V., Chen,Y., Bloom,L., Gokemeijer,J., Shamah,S., Warikoo,V., Wang,J., Ling,V. and Sun,L. (2006) *Chem. Biol.*, **13**, 549–556.

Gilbreth,R.N., Esaki,K., Koide,A., Sidhu,S.S. and Koide,S. (2008) *J. Mol. Biol.*, **381**, 407–418.

Graille,M., Stura,E.A., Corper,A.L., Sutton,B.J., Taussig,M.J., Charbonnier,J.B. and Silverman,G.J. (2000) *Proc. Natl Acad. Sci. USA*, **97**, 5399–5404.

Hackel,B.J., Kapila,A. and Wittrup,K.D. (2008) *J. Mol. Biol.*, **381**, 1238–1252.

Jacobs,S. and O'Neil,K. (2012) In Kaumaya,P. (ed), *FN3 Domain Engineering*. InTech, www.intechopen.com.

Jacobs,S.A., Diem,M.D., Luo,J., Teplyakov,A., Obmolova,G., Malia,T., Gilliland,G.L. and O'Neil,K.T. (2012) *Protein Eng. Des. Sel.*, **25**, 107–117.

Karatan,E., Merguerian,M., Han,Z., Scholle,M.D., Koide,S. and Kay,B.K. (2004) *Chem. Biol.*, **11**, 835–844.

Koide,A., Bailey,C.W., Huang,X. and Koide,S. (1998) *J. Mol. Biol.*, **284**, 1141–1151.

Koide,A., Gilbreth,R.N., Esaki,K., Tereshko,V. and Koide,S. (2007) *Proc. Natl Acad. Sci. USA*, **104**, 6632–6637.

Koide,A., Wojcik,J., Gilbreth,R.N., Hoey,R.J. and Koide,S. (2012a) *J. Mol. Biol.*, **415**, 393–405.

Koide,S., Koide,A. and Lipovšek,D. (2012b) *Methods Enzymol.*, **503**, 135–156.

Krippner-Heidenreich,A., Grunwald,I., Zimmermann,G., *et al.* (2008) *J. Immunol.*, **180**, 8176–8183.

LaPorte,S.L., Juo,Z.S., Vaclavikova,J., Colf,L.A., Qi,X., Heller,N.M., Keegan,A.D. and Garcia,K.C. (2008) *Cell*, **132**, 259–272.

Lehmann,M. and Wyss,M. (2001) *Curr. Opin. Biotechnol.*, **12**, 371–375.

Lehmann,M., Pasamontes,L., Lassen,S.F. and Wyss,M. (2000) *Biochim. Biophys. Acta*, **1543**, 408–415.

Lehmann,M., Loch,C., Middendorf,A., Studer,D., Lassen,S.F., Pasamontes,L., van Loon,A.P. and Wyss,M. (2002) *Protein Eng.*, **15**, 403–411.

Lipovsek,D., Lippow,S.M., Hackel,B.J., Gregson,M.W., Cheng,P., Kapila,A. and Wittrup,K.D. (2007) *J. Mol. Biol.*, **368**, 1024–1041.

Merz,T., Wetzel,S.K., Firbank,S., Pluckthun,A., Grutter,M.G. and Mittl,P.R. (2008) *J. Mol. Biol.*, **376**, 232–240.

Midelfort,K.S. and Wittrup,K.D. (2006) *Protein Sci.*, **15**, 324–334.

Odegrip,R., Coomber,D., Eldridge,B., Hederer,R., Kuhlman,P.A., Ullman,C., FitzGerald,K. and McGregor,D. (2004) *Proc. Natl Acad. Sci. USA*, **101**, 2806–2810.

Olson,C.A., Liao,H.I., Sun,R. and Roberts,R.W.x. (2008) *ACS Chem. Biol.*, **3**, 480–485.

Parker,M.H., Chen,Y., Danehy,F., Dufu,K., Ekstrom,J., Getmanova,E., Gokemeijer,J., Xu,L. and Lipovsek,D. (2005) *Protein Eng. Des. Sel.*, **18**, 435–444.

Pavlou,A.K. and Reichert,J.M. (2004) *Nat. Biotechnol.*, **22**, 1513–1519.

Ramamurthy,V., Krystek,S.R., Jr, Bush,A., *et al.* (2012) *Structure*, **20**, 259–269.

Reichert,J. and Pavlou,A. (2004) *Nat Rev Drug Discov.*, **3**, 383–384.

Richards,J., Miller,M., Abend,J., Koide,A., Koide,S. and Dewhurst,S. (2003) *J. Mol. Biol.*, **326**, 1475–1488.

Schiefner,A., Chatwell,L., Korner,J., Neumaier,I., Colby,D.W., Volkmer,R., Wittrup,K.D. and Skerra,A. (2011) *J. Mol. Biol.*, **414**, 337–355.

Skerra,A. (2000) *J. Mol. Recognit.*, **13**, 167–187.

Sliwkowski,M.X. and Mellman,I. (2013) *Science*, **341**, 1192–1198.

Steipe,B. (2004) *Methods Enzymol.*, **388**, 176–186.

Teplyakov,A., Obmolova,G., Malia,T.J., *et al.* (2013) *Proteins*, doi:10.1002/prot.24502.

Tomschy,A., Brugger,R., Lehmann,M., *et al.* (2002) *Appl. Environ. Microbiol.*, **68**, 1907–1913.

Van den Brulle,J., Fischer,M., Langmann,T., *et al.* (2008) *Biotechniques*, **45**, 340–343.

Wojcik,J., Hantschel,O., Grebien,F., *et al.* (2010) *Nat. Struct. Mol. Biol.*, **17**, 519–527.

Xu,L., Aha,P., Gu,K., *et al.* (2002) *Chem. Biol.*, **9**, 933–942.